Comprehensive Simulation of Surface Texture for End-milling Process

Behnam M. Imani, Ehsan Layegh
Assistant Professor, Graduate Student
Mechanical Engineering Department, Engineering Faculty
Ferdowsi University, Mashad, Iran
Email: imani@um.ac.ir

Abstract
Analysis and simulation of manufacturing process require extensive and complicated computations. But nowadays, computer resources and computational algorithms reach to the state that can model and simulate the problem efficiently. One of the important processes in manufacturing is machining. In this research end-milling process which one of the complex and wide-spread processes in machining is chosen. Most important parameters in end-milling are surface roughness and surface location errors. A comprehensive simulation software is developed to model end-milling process in order to anticipate finishing parameter such as surface roughness and errors. The proposed algorithm take into account cutting conditions, such as feed , doc, woc, tool run out, etc. In addition, dynamic simulation module of the software can accurately model flexible end-mill tool, the milling cutting forces and regeneration of waviness effects in order to construct realistic surface texture model. The software can accurately determine parameter Ra, P.T.V. and surface errors.

Keywords: Machining Simulation, Regeneration, End-milling, Surface Texture, Surface roughness

1. INTRODUCTION

End-milling operations are extensively used in the production of precise part in the industry. Milling process dynamics is investigated in many research works, however due to complexity of the process different fields of research works are required. One area in analyzing and simulation milling process is developing a comprehensive model in order to anticipate surface quality, dimensional error and trend of them in mass production. In various machining process the following steps are required to build up the model:

1- analyzing and modeling machining force
2- modeling dynamic system of machining tool
3- modeling surface generation mechanism

A comprehensive model for accurate anticipation of surface errors requires a "precise" force model. The model must take into consideration phenomena such as, tool deflections, run-out, tool wear, machining dynamics, etc. In the most previous works, machining forces are obtained by mechanistic force model based on oblique cutting tests [1]. In this work, orthogonal cutting theory and transforming method proposed by E.Budak et al is used [2]. In contrast to the previous method, there is no need for oblique cutting test for each tool shape. At first, a general machining data base is provided for orthogonal cutting with various work materials and cutting tool materials. Using transforming relations and tool geometry, cutting coefficients for oblique cutting are determined.

In general, one of the important sources of vibrations in milling process is self-excited vibration. In this kind of vibrations, internal sources will provide energy for the system. In some cases, the energy will exceed damping thus vibrations sustain or even grow in amplitude. One of the important principles observed in machining dynamics is the regeneration of waviness affecting chip thickness [3].

In current research, a dynamic simulation model for machining dynamics is proposed. Then, surface are modeled using a 3D algorithm which an extension to available 2D methods. The developed simulation model can anticipate surface rough in any direction of interest on the machined surface.

2. CUTTIN FORCES SIMULATION

Figure 1-a and 1-b illustrate coordinate system and end-milling geometry required for the model. Differential forces, df_t tangential, df_r radial and df_a axial are depicted which act on jth cutting edge for an ideal system (with out any deflection). Values of the differential forces are obtained by:

$$\begin{aligned} df_{tj}(\theta,z) &= \left[K_{te} + K_{tc}h_j(\theta,z)\right]dz \\ df_{rj}(\theta,z) &= \left[K_{re} + K_{rc}h_j(\theta,z)\right]dz \\ df_{aj}(\theta,z) &= \left[K_{ae} + K_{ac}h_j(\theta,z)\right]dz \end{aligned} \quad (1)$$

In equations (1) there are two separate terms, the first one is related to friction and ploughing force and the second term is considered for the cutting action which taks place in the shear zone. coefficients for the first phenomena are represented by K_{te}, K_{re}, K_{ae} showing amont of force per unit length of the cutting edge. Coefficients represented by K_{tc}, K_{rc}, K_{ac} are considered for cutting action showing amunt of force per unie area of cutting edge.

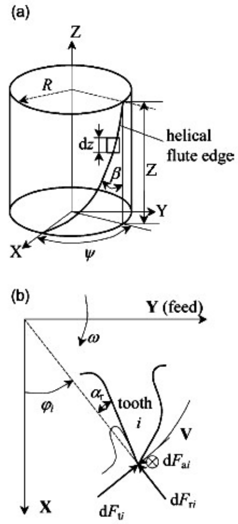

Figure 1 coordinate system and end-milling geometry

MATLAB code is written to compute cutting and edge force coefficients and then the code computes cutting forces. Table 1 summarizes computed coefficients for a four-flute HSS tool and aluminium work-piece 7075-T6 with yield stress of 542 Mpa. Computed cutting forces are depicted in Figure 2.

Table1 computed coefficient for a four-flute HSS tool and aluminium work-piece 7075-T6 with yield stress of 542 Mpa

α_n (deg)	K_{tc} [N/mm^2]	K_{rc} [N/mm^2]	K_{ac} [N/mm^2]
0	1642.3	609.5	512.2
12	1396.2	519.8	258.1
15	1356.5	504.4	215.3

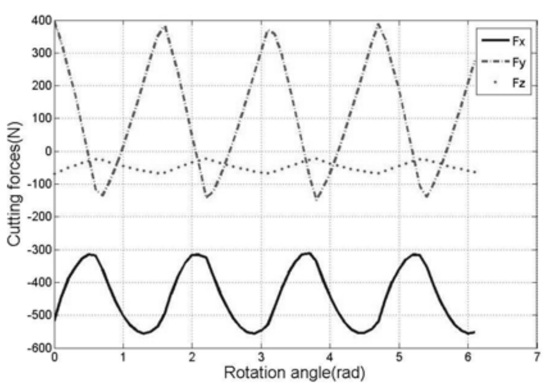

Figure 2 simulated cutting forces for a four-flute HSS tool and aluminium work-piece 7075-T6 with yield stress of 542 Mpa. Cutting conditions are d=10mm, f_t= 0.05mm/tooth, doc=10mm

3. REGENERATION OF WAVINESS

Almost in every machining process, the tool is cutting a surface which generated in the previous passes. If there exists any vibrations between tool and work piece, the newly generated surface undulates and results in the variation of chip thickness. Figure 3 illustrate the model used for simulation of milling process. Dynamic characteristic of the system in x and y direction is also depicted. Differential forces can be obtained by:

$$dF_{t_{n+1}} = K_{tc} da(h_0 - z_n + zold1 + zold2 + zold3)$$
$$dF_{r_{n+1}} = K_{rc} da(h_0 - z_n + zold1 + zold2 + zold3) \quad (2)$$

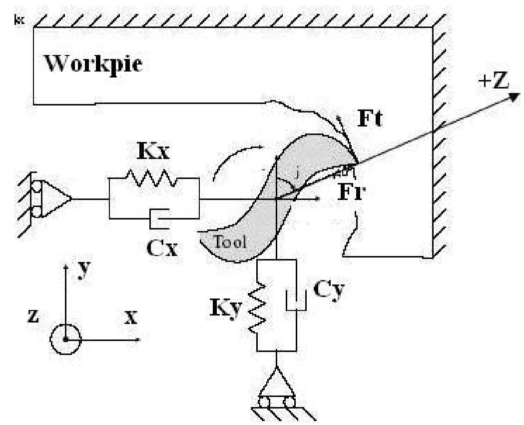

Figure 3 model used for simulation of dynamic milling process

Due to the fact that axial stiffness of the tool and the spindle assembly is high and also axial force is smaller than others, axial vibrations are ignored. In above relations, n, h_0, z, zold1 to zold3 and da in order are: index of time increment, nominal chip thickness, tool deflection normal to the cut surface, tool deflection in previous passes and axial increment. At each instance, differential cutting forces on engaged cutting edges are computed and projected on X and Y axis. Then the total cutting forces are the summation of differential forces over engaged edges. Using Newton's second law differential equations of motion is written then by double Euler integration dynamic deflections are obtained.

$$F_{x_{n+1}} = m\ddot{x}_n + C\dot{x}_n + Kx_n$$
$$F_{y_{n+1}} = m\ddot{y}_n + C\dot{y}_n + Ky_n \quad (3)$$

Where m, K and C are mass, stiffness and damping matrices, respectively.
Input data for a four flute end-mill with helix angle of 30° are considered as follows [3]:

$$f_x = f_y = 660HZ$$
$$K_x = K_y = 2\times10^7 N/m$$
$$M_x = K_x/(2\pi f_x), My = K_y/(2\pi\ f_y)$$

$$\eta_x = \eta_y = 0.05$$

$$C_x = \eta_x \times 2\sqrt{K_x M_x}, C_y = \eta_y \times 2\sqrt{K_y M_y}$$

$$r = 5mm,\ n = 1200\,rpm,\ doc = 10mm$$

Nominal cheap thickness at angular position θ is:

$$h_0 = ft \times Sin\theta \quad (5)$$

and normal to cut deflection is :

$$Z_n = x_n Sin\theta + y_n Cos\theta \quad (6)$$

One of the advantages of the proposed model is that it is possible to include non-linear ties such as jump-of-cut into the model. Figure 4 shows the simulation results for aluminium 7075-T6 work piece. Cutting conditions are as follow:
d = 10 mm, h = 30deg, ft = 0.1 mm/tooth, woc = 1.2 mm, n = 1200 rpm, doc= 10 mm.
Dynamic milling forces for woc = 3 mm are shows in Figure 5. Fourier transform of the milling forces are computed and depicted in Figure 6.
Dominant frequency in the stable cutting is tooth passing frequency, however as inferred from Figure 6 the dominant frequency in the unstable cutting is close to natural frequency of flexible mode shape, known as chatter frequency. At this cutting condition, milling is unstable and vibration grows in amplitude gradually.

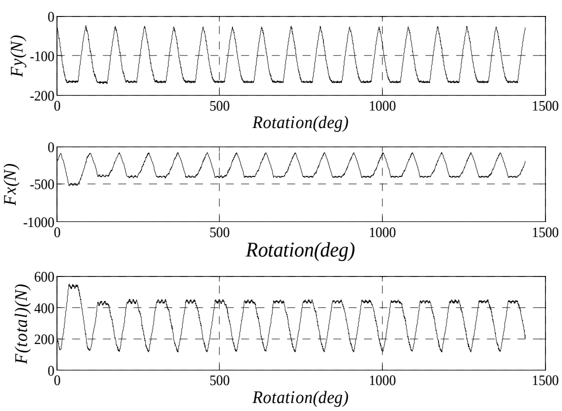

Figure 4 dynamic simulation of cutting forces for aluminium 7075-T6 work piece. Cutting conditions are: d = 10 mm, h = 30deg, ft = 0.1 mm/tooth, woc=1.2

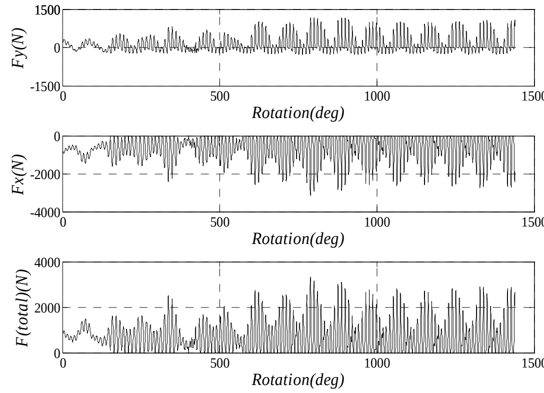

Figure 5 dynamic simulation of cutting forces for aluminium 7075-T6 work piece. Cutting conditions are : d = 10 mm, h = 30deg, ft = 0.1 mm/tooth, woc=3mm

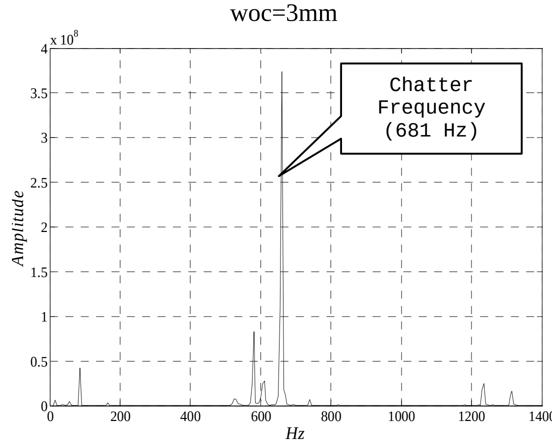

Figure 6 Fourier transform of the milling forces

4. DYNAMIC VIBRATIONS OF THE TOOL AND SPINDLE

Surface roughness prediction module requires a comprehensive model in time domain witch can simulate tool vibrations at locations of interest on the work piece. In the current research milling vibration are modeled by FEM using CALFEM toolbox implemented in MATLAB software [4].
Figure 7 schematically shows the mesh generated for the end-mill and spindle assembly, which modeled as a step beam and two simple supports.

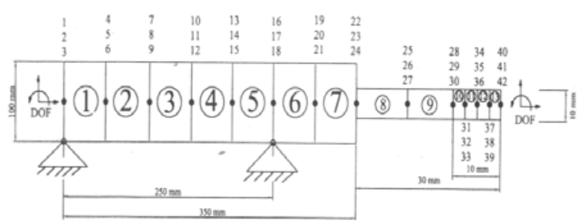

Figure 7 mesh generated for the end-mill and spindle assembly

Axial variation of the tool deflection is required for the engaged portion of tool in order to be used by the surface location error algorithm. Thus, finer elements at this portion are introduced to get deflection variations..
Inputs for FE analysis are given in following:

module of elasticity = 207×10^9 (N/m^2), inner diameter of spindle axis = 0.02 m, outer diameter of spindle axis = 0.1 m, density = 7800(Kg/m^3).

Figure 8 illustrates the developed flowchart of the FE analysis. Input to the algorithm is tool radius, chip width, cheep depth, feed, cutting force constants and spindle speed. BMCK function calculates mass, stiffness and damping matrices. This function is written in MATLAB 7.0 and uses pre-defined functions of CALFEM toolbox. Using mesh and node positions, mass, stiffness and damping of each element are computed and then assembled together to get overall matrices. In addition boundary conditions and external cutting forces are applied. Differential equations of motion are integrated numerically by Newmark method.

$$\begin{cases} M\ddot{X} + C\dot{X} + KX = F_X \\ M\ddot{Y} + C\dot{Y} + KY = F_Y \end{cases} \tag{7}$$

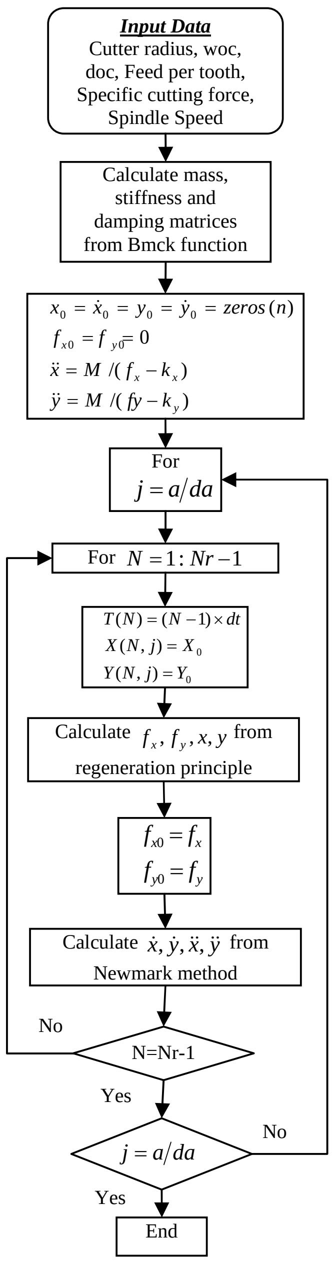

Figure 8 developed flowchart of the FEM analysis

Initial values of displacements and velocities are set to zero, but value of initial acceleration computed by following relation:

$$\ddot{X} = \frac{M}{(F_x - K_x)} \quad , \quad \ddot{Y} = \frac{M}{(F_y - K_y)} \tag{8}$$

The iteration loop starts from 1 and end to a/da (where a is DOC and da is axis increment), thus the variation of axial deflection is obtained. Counter N varies from 1 to Nr-1 which is considered for the time increments. After computing F_x, F_y, x, and y at current time increment, these values are used as initial values for the next step.

In the Figure 9, results of time domain FE analysis of the milling tool is shown. Vibrations of the tool center point are plotted at constant axial levels.

In the next section amount of vibrations is used for determining cutting edge position and surface generation method.

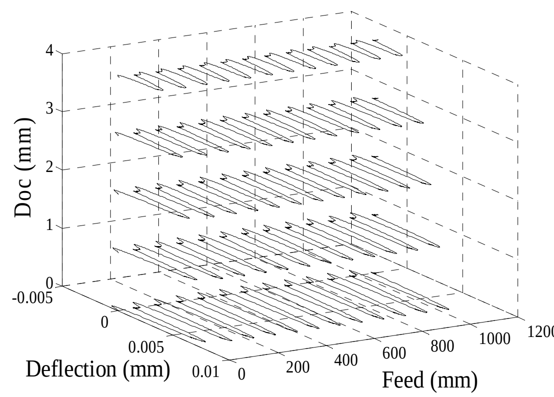

Figure 9 results of time domain FE analysis of the milling tool for d= 12 mm, f_t=0.3 mm/tooth, K_{tc}=2000N/mm^2, doc=5mm, woc=1.5 mm

5. SURFACE ROUGHNESS SIMULATION

Final machined surface is produced by subsequent cutting actions of end-mill cutting edges. Ideally points on the cutting edge have trochoidal paths which leave feed marks on the surface. Additionally, any tool deflection, vibrations or geometric error results in undesirable deformation and deteriorate required surface roughness on the work piece. Ideal position of the cutting edges with respect to tool cutter is shown in Figure10.

As illustrated coordinate system XOY is attached to the work piece and original O is on the initial center position of the spindle.

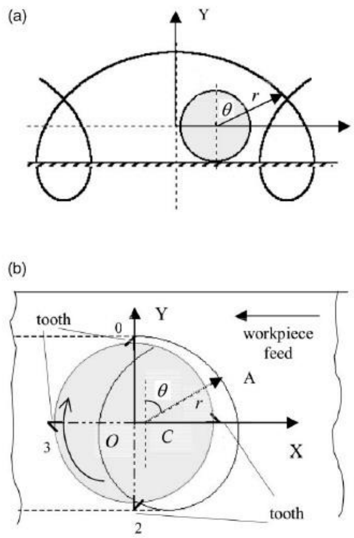

Figure 10 Trochoidal path of a point on cutting edge

Trochoidal motion of the point on the cutting is computed by bellow relation:

$$X_{l/c}(i,z,t) = R\sin(\theta(t) - \psi(i) - \alpha(z))$$
$$Y_{l/c}(i,z,t) = -R\cos(\theta(t) - \psi(i) - \alpha(z)) \qquad (9)$$

where $X_{l/c}$ and $Y_{l/c}$ are coordinate of the edge with respect to tool center point. Also *i*, *r*, $\theta(t)$, $\psi(i)$, $\alpha(Z)$ in order are tooth index, tool radius, angular position of the lowest point of the reference cutting edge, pitch angle and phase lag of the point at higher levels. $\alpha(Z)$ is given by:

$$\alpha(Z) = \frac{z\tanh}{R} \qquad (10)$$

Where h is tool helix angle.
On the other hand, displacement of spindle center with respect to work piece can be found by:

$$X_{s/w} = f_r \times \theta(t)/(2\pi) \qquad (11)$$

If there exists the runout error, the location of tool center with respect to spindle axis can be found by:

$$Y_{c/s}(t,z) = -\rho \times \cos(\theta(t) + \lambda) + Y_{FEM}(t,z)$$
$$X_{c/s}(t,z) = \rho \times \sin(\theta(t) + \lambda) + X_{FEM}(t,z) \qquad (12)$$

Where ρ is runout offset and λ is its angular position, refer to Figure 11.

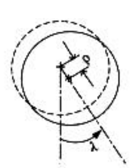

Figure 11 runout parameters

$X_{FEM}(t,z)$ and $Y_{FEM}(t,z)$ are dynamic tool deflections at time t and z level, which are calculated by FE analysis.
Thus, path of points of the cutting edge are:

$$X_{l/w} = X_{l/c} + X_{c/s} + X_{s/w}$$
$$Y_{l/w} = Y_{l/c} + Y_{c/s} + Y_{s/w} \qquad (13)$$

Figure 12 shows trochoidal motion of the cutting edges without considering vibrations and runout.
In order to shows effects of the runout, its value is set to 1mm, which is exaggerated intentionally. The other cutting conditions are kept constant. The simulation results are shown in Figure 13.
Finally, Figure 14 shows path of cutting edge including tool vibrations.

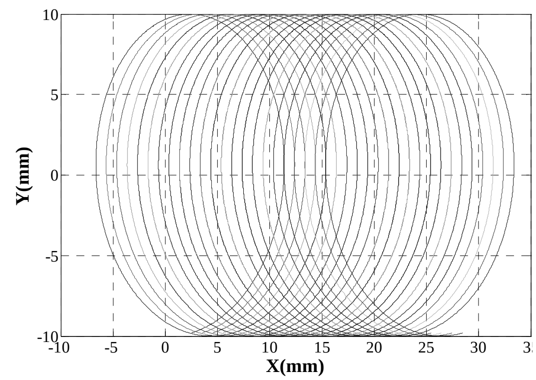

Figure 12 trochoidal motions of the cutting edges without considering vibrations and runout (f_t=1mm/tooth, d=20mm)

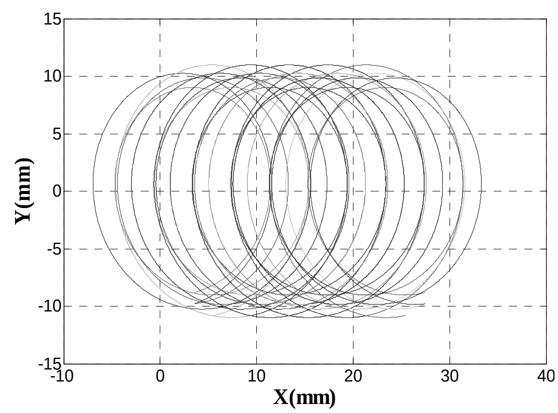

Figure 13 trochoidal motions of the cutting edges with considering exaggerated runout

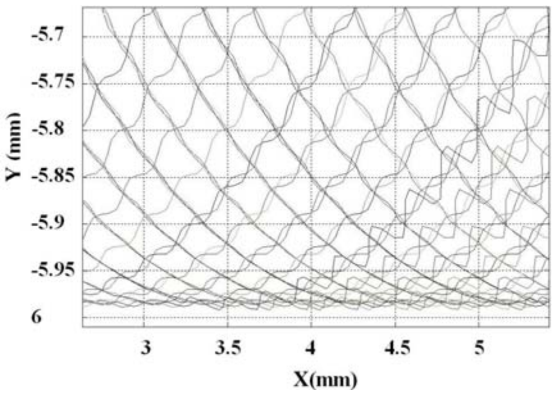

Figure 14 trochoidal motions of the cutting edges with considering vibrations (d=12 mm, f_t=0.3 mm/tooth)

6. SURFACE TEXTURE

Final produced surface can be represented as follows. Points on the computed paths which do not make contact with newly generated surface are deleted by the algorithm Figure 15, 16, 17 illustrate 3D surface model which interpolates z level profiles for different cutting conditions. Cutting condition of Figure 15 result in very limited vibrations. Figure 16 shows the generated surface when there is tool runout. Lastly, Figure 17 shows the simulation surface texture when there exists excessive vibrations of the tool.

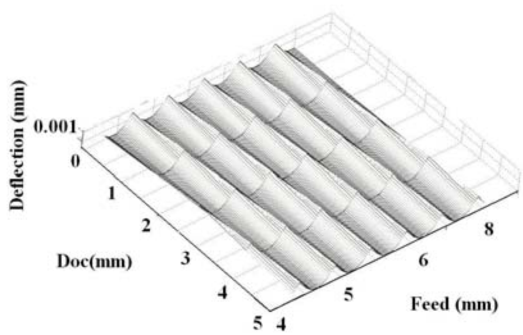

Figure 15 surface texture for d=12mm, woc=1mm, doc=5mm, f_t=0.1mm/tooth, K_{tc}=1500 N/mm^2 (Ra=1.4 μ)

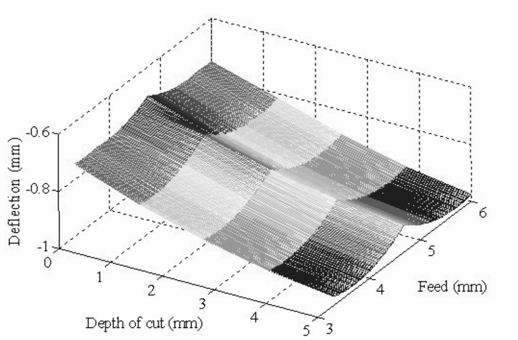

Figure 16 surface texture for d=10mm, woc=1mm, doc=5mm, f_t=0.1mm/tooth, K_{tc}=1500 N/mm^2, ρ =1mm (Ra=3.5 μ)

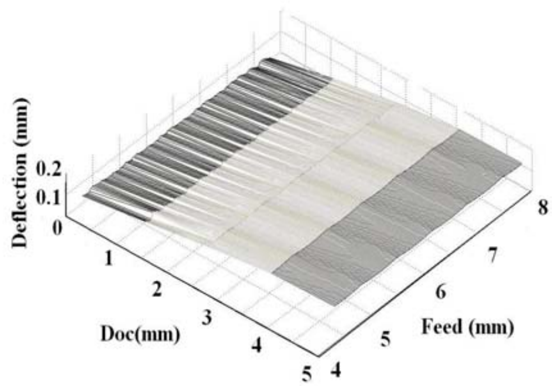

Figure 17 surface texture for d=12mm, woc=4.5mm, doc=5mm, f_t=0.6mm/tooth, K_{tc}=1500 N/mm^2, ρ =0.01mm (Ra=14 μ)

As shown, amplitude of vibrations at the tool tip is much higher.

Table 2 summarizes Ra values of surface roughness computed at tool tip.

Table 2 surface roughness computed at tool tip.

d (mm)	a (mm)	WOC (mm)	ft (mm/tooth)	Ra μ
10	5	1.0	0.05	1.14
10	5	1.5	0.1	3.99
10	5	1.5	0.25	5.85
12	5	1.5	0.1	2.24
12	5	2	0.1	3.07
12	5	3	0.15	4.61

7. CONCLUTIONS

In this research work a comprehensive simulation model is developed for anticipating dynamic cutting forces and 3D surface texture for end-milling operations. Dynamic deflections of the tool are computed by FE analysis using CALFEM toolbox implement in MATLAB environment. Variations of dynamic tool deflections are also computed along axial direction, In order to construct 3D surface texture model. The final model contains all information required to compute surface roughness parameter and surface location errors.

REFERENCES

Journal article:

[1] E.Budak and Y.Altintas, (1992) "Flexible Milling Force Model for Surface Error Prediction", *Proceeding of the Engineering System Design and Analysis*, Istanbul, Turkey, pp. 89-94

[2] E.Budak, Y.Altintas, E.J.A.Armarego, (1996) "Prediction of Milling Force Coefficient from

Orthogonal Cutting Data", 1st ed., *Cambridge University Press*, NY, USA.

[3] S.Smith, and J.Tlusty (1991), "An Overview of Modelling and Simulation of Milling Process", ASME Journal of Engineering for Industry, vol.113, No.2, pp.169-175.

[4] "CALFEM, A Finite Element Toolbox," V3.3, *LUND University*, Sweden

[5] D. Montgomery, and Y.Altintas, (1991) "Mechanism of Cutting Force and Surface Generation in Dynamic Milling", ASME Journal of Engineering for Industry, vol.113, pp.160-168.

[6] Y. Altintas, D. Montgomery, E. Budak, (1992) "Dynamic Peripheral Milling of Flexible Structures", ASME Journal of Engineering for Industry, vol. 114/137, pp. 137-145,

Book:

[7] Altintas, Y., (2000) "Manufacturing Automation, Metal Cutting Mechanics, Machine Tool Vibration and CNC Design," *Cambridge University Press*.

[8] Jiri Tlusty, (2000) "Manufacturing Process and equipment", Prentice Hall, New Jersey